



Effect of tensile and compressive strain on the magnetic ordering of the $(\text{LaMnO}_3)_1/(\text{SrTiO}_3)_1$ superlattice

A AEZAMI

Department of Physics, Ahvaz Branch, Islamic Azad University, Ahvaz, Iran
E-mail: a.aezami@gmail.com

MS received 9 July 2017; revised 7 January 2018; accepted 8 January 2018; published online 19 June 2018

Abstract. We study the effects of tensile and compressive strain on the $(\text{LaMnO}_3)_1/(\text{SrTiO}_3)_1$ superlattice from density functional theory using Quantum-Espresso open source code. In the unstrained superlattice, electron interactions in out-of-plane Mn–O–Ti chains are dominated by superexchange interactions, giving rise to ferromagnetic and half-metallic conducting characters. We found that the most stable magnetic configuration is G-type antiferromagnetic configuration for strong compressive strain and for strong tensile strain it is A-type antiferromagnetic configuration. The results are in accordance with the experimental observations which show that the superlattices can be grown on different substrates, and due to the difference in lattice parameters of the substrate and the main layer, there are also changes in the amount of strain applied to the superlattice.

Keywords. Superlattice supercell; $(\text{LaMnO}_3)_1/(\text{SrTiO}_3)_1$ superlattices; density functional theory; tensile strain; compressive strain.

PACS Nos 71; 73; 75

1. Introduction

New advances in designing interfaces between dissimilar transition metal oxides have revealed the formation of their parent compounds which have applications in spintronics [1]. The interfacial properties show that various magnetic and electronic structures are due to the coupling between degrees of freedom such as charge, spin and orbital. For example, the magnetic ordering at the interface between the two insulators LaMnO_3 (antiferromagnetic, A-type) and SrTiO_3 (paramagnetic) could be ferromagnetic [2,3]. These changes can depend on the epitaxial strain on the interface. By applying strain, the orbital ordering changes causing the magnetic properties of the interface layer in the superlattices to vary [4]. In this investigation, we consider the effects of external strain on the magnetic ordering of the $(\text{LaMnO}_3)_1/(\text{SrTiO}_3)_1$ superlattice (labelled SL1-1). We have applied different external strains ($\varepsilon_1 = \pm 5\%$ and $\varepsilon_2 = \pm 10\%$) along the z -axis. We have compared unstrained superlattices (the superlattices without the external strain) with superlattices that have been affected by external strain.

We have considered two external strains, which include tensile strain (TS) if $\varepsilon > 0$ and compressive strain (CS) if $\varepsilon < 0$.

2. Structural and computational details

We have studied the effects of external strain on the magnetic ordering of the $(\text{LaMnO}_3)_1/(\text{SrTiO}_3)_1$ superlattice (SL1-1) using density functional theory calculations. We have grown SL1-1 superlattice from first principle calculation by using the Quantum-Espresso within LDA+U approaches [5]. We have applied a strong Coulomb repulsion U on the Mn and Ti atoms with moderate value of 3.5 eV and 5 eV, respectively, in our superlattice. We have calculated Hubbard U with linear response approach [6] using the wave pseudopotential method implemented in Quantum-Espresso code for Mn and Ti in LaMnO_3 and SrTiO_3 , respectively, and it is in accordance with other reported calculations. A linear response approach is proposed that is internally consistent with the chosen definition of the occupation matrix of the relevant localised orbitals.

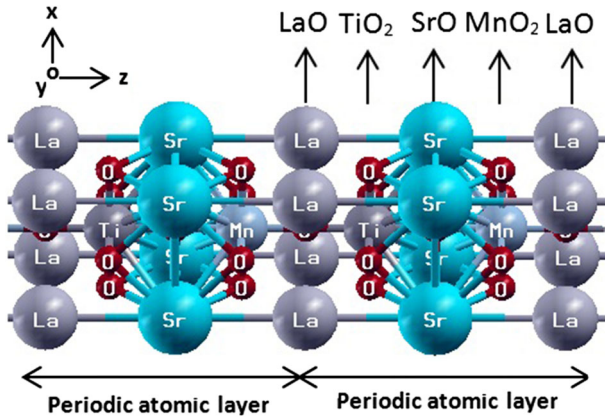


Figure 1. Structure of periodic atomic layer in the SL1-1 superlattice along the z -axis.

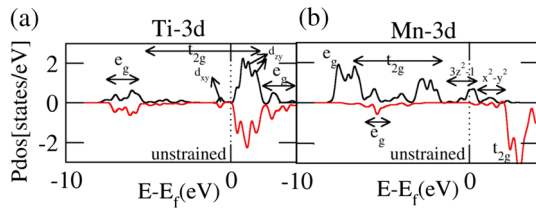


Figure 2. Partial DOSs of Ti-3d atom (a) and Mn-3d atom (b) in the SL1-1 superlattices. The Fermi energy is denoted by the vertical dotted line.

The unit cell of the SL1-1 superlattice is created on the basis of the relaxed cubic perovskite structures of LaMnO_3 and STiO_3 , with lattice parameters of 3.879 \AA and 3.911 \AA , respectively [3].

The energy cut-off of 30 Ry was set for the plane-wave expansion. We have taken the xy -plane lattice parameters of SL1-1 superlattice coinciding with calculated lattice constraints of the LaMnO_3 bulk and the out-of-plane lattice parameters (c) are taken to be 3.976 \AA and 3.879 \AA for SrTiO_3 and LaMnO_3 respectively, while preserving unit cell volumes [7]. Figure 1 schematically shows a prototype of SL1-1 superlattice.

3. Result and discussions

In this investigation, we describe the effect of strain on the electronic structure at the interface of the $(\text{LaMnO}_3)_1/(\text{SrTiO}_3)_1$ superlattices from DFT calculations. Furthermore, we resolve the partial density of state of the unstrained SL1-1 superlattice (see figure 2).

In SL1-1 unstrained superlattice, the Mn e_g state orbitals ($x^2 - y^2$ and $3z^2 - 1$ orbitals) are nearly degenerate. Both these orbitals have states on the Fermi surface (figure 2), thus allowing electron transport along the

Table 1. Calculated total energies for different magnetic configurations of SL1-1 superlattice without strain (unstrained), with compressive strain ($\epsilon_1 = -5\%$ and $\epsilon_2 = -10\%$) and with tensile strain ($\epsilon_1 = +5\%$ and $\epsilon_2 = +10\%$). All energies are normalised to a ferromagnetic ordering energy.

SL1-1	FM	A-AFM	C-AFM	G-AFM
Unstrained	0	0.841	0.285	0.299
ϵ_1 CS	0	0.612	0.258	-0.244
TS	0	-0.383	0.244	0.244
ϵ_2 CS	0	0.381	0.145	-0.153
TS	0	-0.172	0.181	0.190

Mn–O–Mn and Mn–O–Ti chains in all x -, y - and z -axes, respectively. The Mn t_{2g} state orbitals (d_{xy} , d_{xz} , d_{yz}) completely filled, thus do not contribute to electron conduction. In addition, we have constructed supercells for this superlattice along x - and z -axes which are called superlattice supercell. We have calculated the Mn–Ti exchange interaction energy ($J = E_{\downarrow\downarrow} - E_{\uparrow\downarrow}$), using density functional theory within LDA+U approximation with $U_{\text{Mn}} = 3.5 \text{ eV}$ and $U_{\text{Ti}} = 5 \text{ eV}$. The results show that in SL1-1 superlattice supercell, the exchange interaction energies between Ti–Ti atoms and Mn–Mn atoms along the x -axis are -3.1 meV and -2.8 meV , respectively. The exchange interaction energies between Mn–Mn, Ti–Ti and Mn–Ti atoms along the z -axis are -4.9 meV , -1.4 meV and -2.01 meV , respectively. The exchange interaction energies for neighbouring atoms in the SL1-1 superlattice supercell (unstrained) are negative and ferromagnetic. The results in table 1 show that e_g electron interactions in the Mn–O–Ti chains are dominated by superexchange interactions, which give rise to ferromagnetic and half-metallic conducting characters of the SL1-1 unstrained superlattice. In table 1, it is shown that for a strong compressive strain, ‘G-type’ is the most stable magnetic configuration, and for a strong tensile strain ‘A-type’ is the most stable magnetic configuration. We observe that if strain changes, the occupancy at the e_g orbitals will change (shown in table 1).

According to figure 3, application of the TS compresses the MnO_6 and TiO_6 octahedrals along the z -axis. It is obvious that only electrons in the lower energy $x^2 - y^2$ orbitals of Mn and the $2p_x$ and $2p_y$ orbitals in plane O atoms, O_x and O_y , respectively, contribute to the Fermi level, resulting in two-dimensional electron transport in the xy directions. However, conduction electrons, occupying the $x^2 - y^2$ orbitals to develop a strong double exchange in the x - and y -axes direction Mn–O–Mn chains, yield xy -plane ferromagnetic configuration. The immobile $3z^2 - 1$ electrons favour superexchange

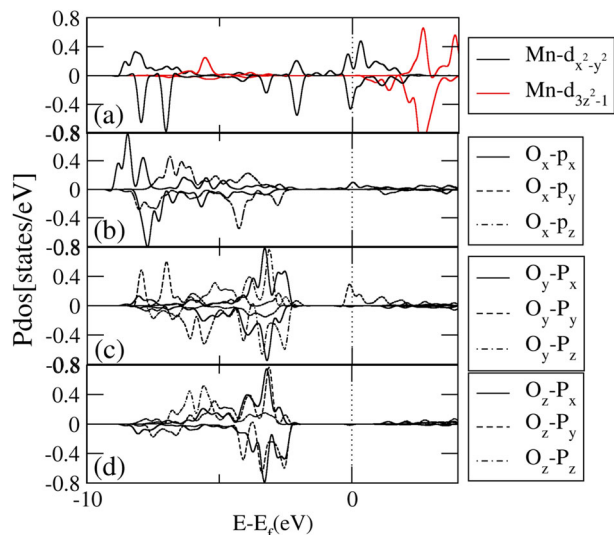


Figure 3. Partial DOSs of the $\text{Mn-}d_{x^2-y^2}$ and $\text{Mn-}d_{3z^2-1}$ (a), partial DOSs of the $\text{O}_x - \text{P}_x$, $\text{O}_x - \text{P}_y$ and $\text{O}_x - \text{P}_z$ (b), partial DOSs of the $\text{O}_y - \text{P}_x$, $\text{O}_y - \text{P}_y$ and $\text{O}_y - \text{P}_z$ (c), partial DOSs of the $\text{O}_z - \text{P}_x$, $\text{O}_z - \text{P}_y$ and $\text{O}_z - \text{P}_z$ (d), of the SL1-1 superlattice with compressive strain ($\varepsilon_1 = -5\%$). Application of the CS causes only electron in the lower energy $x^2 - y^2$ orbitals of Mn and the $2p_x$ and $2p_y$ orbitals of in-plane O_x and O_y , respectively. The Fermi energy is denoted by the vertical dotted line.

(Mn–O–Ti chains), which develop a strong antiferromagnetic configuration along the z -axis. This type of antiferromagnetic order is called A-type antiferromagnetic order.

For the unstrained structure, both e_g orbitals are more or less equally occupied. In the LaMnO_3 bulk, Mn^{3+} atom has the electronic configuration $t_{2g}^3 e_g^1$ and in the bulk SrTiO_3 , Ti^{4+} atom has the electronic configuration $t_{2g}^3 e_g^0$. As the MnO_2 layers are surrounded by $(\text{SrO})^0$ layer and $(\text{LaO})^+$ layer, at the interface Mn and Ti atom are left with the average valance state of +3.5. The t_{2g} orbitals will be occupied by three electrons in the spin majority states and the e_g orbitals will be occupied by the remaining 0.5 electrons.

In the partial density of states in figure 4, the application of CS stretches the MnO_6 and TiO_6 octahedra along the z -axis and removes the degeneracy of the e_g states of the Mn atom via the Jahn–Teller effect, splitting them into the higher energy $x^2 - y^2$ and the lower energy $3z^2 - 1$ orbitals [3]. Here, one can see that only electrons in the $3z^2 - 1$ orbitals of Mn and $2p_z$ orbitals in the z -axis of O atoms have states on the Fermi surface. Electron transport is therefore one-dimensional, along the Mn–O–Ti chains in the z -axis. Simultaneously, these conduction electrons in the $3z^2 - 1$ orbitals cause a superexchange interaction along the z -axis direction of Mn–O–Ti chains, resulting

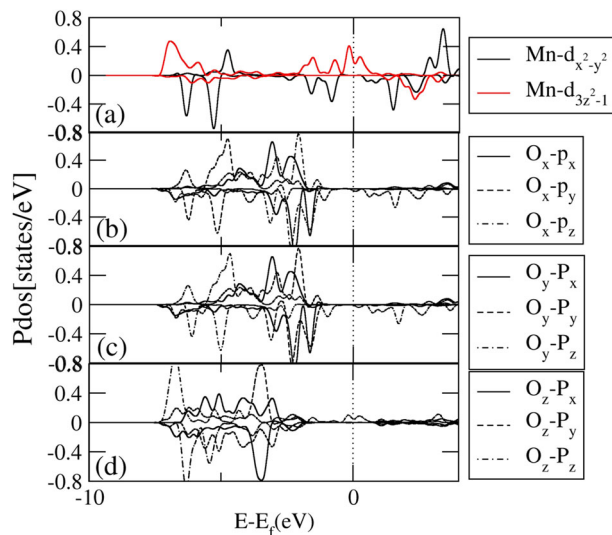


Figure 4. Partial DOSs of the $\text{Mn-}d_{x^2-y^2}$ and $\text{Mn-}d_{3z^2-1}$ (a), partial DOSs of the $\text{O}_x - \text{P}_x$, $\text{O}_x - \text{P}_y$ and $\text{O}_x - \text{P}_z$ (b), partial DOSs of the $\text{O}_y - \text{P}_x$, $\text{O}_y - \text{P}_y$ and $\text{O}_y - \text{P}_z$ (c), partial DOSs of the $\text{O}_z - \text{P}_x$, $\text{O}_z - \text{P}_y$ and $\text{O}_z - \text{P}_z$ (d), of the SL1-1 superlattice with tensile strain ($\varepsilon_1 = +5\%$). Application of the TS causes only electron in the lower energy $3z^2 - 1$ orbitals of Mn and $2p_z$ orbitals of the z -axis direction O atoms. The Fermi energy is denoted by the vertical dotted line.

in plane antiferromagnetic ordering along the z -axis direction. The immobile $x^2 - y^2$ electrons meanwhile favours the superexchange resulting in a strong xy -plane antiferromagnetic ordering which is called G-type antiferromagnetic ordering, according to the results in table 1.

The results show that our superlattice is without external strain (unstrained superlattice) and has a ferromagnetic order. Table 1 confirms this. If external strain is applied along the z -axis, magnetic order will change. As a result of applying the strain along the z -axis, the magnetic ordering becomes antiferromagnetic. As seen in figures 5 and 6, without external strain superlattice electrically have half-metal and show a 100% polarisation. As calculations show that by applying external strain can be seen in the metallic properties and reduce spin polarisation of superlattice. Figures 5 and 6 show that in SL1-1 superlattice with increasing external strain along the z -axis from 5% to 10%, the electric and magnetic properties change similarly.

The results significantly show that the superlattice can be grown on different substrates and due to the difference in lattice parameters of substrates and main layers, there are also changes in the amount of strain applied to the superlattice. For example, we have calculated that if the SrTiO_3 substrate is selected according to the calculations made, the c

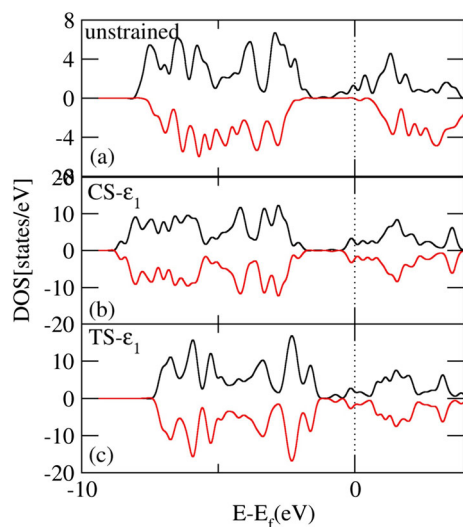


Figure 5. Comparison of total density of states for the SL1-1 superlattice without strain (unstrained) (a), with compressive strain ($\epsilon_1 = -5\%$) (b) and with tensile strain ($\epsilon_1 = +5\%$) (c).

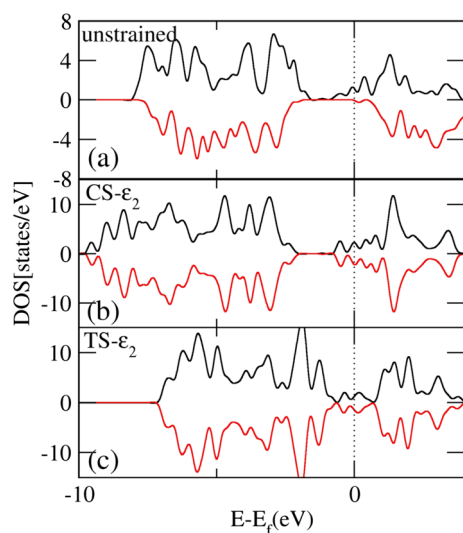


Figure 6. Comparison of total density of states for the SL1-1 superlattices without strain (unstrained) (a), with compressive strain ($\epsilon_2 = -10\%$) (b) and with tensile strain ($\epsilon_2 = +10\%$) (c). The Fermi energy is denoted by the vertical dotted line.

parameter in the layers of the superlattice would be determined to be 3.787 Å (Mn–O distance) and 3.976 Å (Ti–O distance). In addition, if the LaAlO₃ substrate is selected, c parameters will be 4.066 Å (Mn–O distance) and 4.167 Å (Ti–O distance).

The results show that when the substrates are LaMnO₃ ($c/a \cong 1$), SrTiO₃ ($c/a < 1$) and LaAlO₃ ($c/a > 1$), the respective magnetic configurations at the (LaMnO₃)_m/(SrTiO₃)_n superlattice interfaces change.

4. Conclusions

In summary, we have calculated both the tensile strain and compressive strain on the electronic structure at the interface of the (LaMnO₃)₁/(SrTiO₃)₁ superlattices from DFT calculations. By calculating the total energies for different magnetic configuration of SL1-1 superlattice, we found that the magnetic configurations without strain (unstrained) are ferromagnetic, the magnetic configurations with compressive strain ($\epsilon_1 = -5\%$ and $\epsilon_2 = -10\%$) are G-type antiferromagnetic and magnetic configurations with tensile strain ($\epsilon_1 = +5\%$ and $\epsilon_2 = +10\%$) are A-type antiferromagnetic. The results show that the changes in strain cause the occupancy of electrons in the e_g orbitals which controls the magnetic interaction at the interface. Furthermore, the results show that the strain changes by changing the substrates.

Acknowledgements

The authors thank Dr M Niyafar from Ahvaz Branch, Islamic Azad University for support and helpful discussions.

References

- [1] F Cossu, N Singh and U Schwingenschlogl, *Appl. Phys. Lett.* **102**, 042401 (2013)
- [2] J G Barriocanal *et al*, *Nat. Commun.* **1**, 82 (2010)
- [3] A Aezami, M Abolhassani and M Elahi, *J. Alloys Compd.* **587**, 778 (2014)
- [4] B R K Nada and S Satpathy, *Phys. Rev. B* **78**, 054427 (2008)
- [5] P Giannozzi *et al*, *J. Phys.: Condens. Matter* **21**, 395502 (2009)
- [6] M Cococcioni and S de Gironcoli, *Phys. Rev. B* **71**, 035105 (2005)
- [7] R B K Nada and S Satpathy, *Phys. Rev. B* **79**, 054428 (2009)